Structural Chemistry
https://doi.org/10.1007/s11224-024-02312-6

RESEARCH

Determination of dissociation constants of cephalosporin antibiotics by cellmetry method

Malek Sadatsharifi[1] · **Mihály Purgel**[1]

Received: 13 February 2024 / Accepted: 13 March 2024

Abstract
Acid dissociation constants of three cephalosporin antibiotics (cefapirin, ceftiofur, and cefotaxime) were calculated by a newly developed methodology. Plane-wave DFT calculations were performed to determine the pK_a values, and by choosing the appropriate cell sizes, accurate values could be calculated. Some characteristic points were found which helped us to find correlations among the structural and physic-chemical parameters, and correlation factors were defined as well. This present study can be a base for further approaches to determining acid dissociation constants of cephalosporin molecules.

Keywords Prediction · ß-Lactam antibiotics · Veterinary medicine · Accuracy · Data analysis

Introduction

There are different generations of cephalosporin ß-lactam antibiotics which show a broad activity against Gram-positive and Gram-negative bacteria as well as different kinds of resistance to hydrolysis by ß-lactamase [1–3]. The cephalosporins have similar central structures, but a wide range of additional functional groups can vary their properties due to the combination of the "two-side" modifications. In this work, three cephalosporins were studied: both first-generation cefapirin (CEFA) and third-generation ceftiofur (CEF) have one side which is as same as in the third-generation cefotaxime (CEFO), see Fig. 1. CEFA and CEF are used as antibiotics in veterinary medicine, while CEFO has a broader range of usage, especially in the agricultural industry regarding its more complex structure and functionalities [4–6]. Their neutral form is known as a zwitter ion since the proton can be stabilized by the heterocyclic rings [7, 8].

The ionic forms depending on the pH can be different; therefore, it is necessary to obtain their pK_a values which show a wide range dependent on the method that was used for determining them [9–12]. Some predictors like Marvin developed by ChemAxon or ACD/Percepta by Advanced Chemistry Development packages result in accurate values based on a wide range of molecular structures using empirical statistic algorithms derived from experimental pK_a values [13, 14].

One of the possible ways to determine pK_a values is the empirical pK_a calculation method [15, 16], where from the reaction free energies of the acid/base dissociations (Eqs. 1, 2, 3, and 4), the dissociation constant can be calculated (Eq. 5) by an additional experimental term (−1.74) that corrects the standard state of liquid water of 55.5 mol L^{-1} (−log55.5) where the * denotes the standard state of 1 mol L^{-1}.

$$HA(aq, 1M) + H_2O\ (1, 1M) \rightarrow H_3O^+(aq, 1M) + A^-(aq, 1M) \quad (1)$$

$$\Delta G^*_{Diss} = G(A^-) - G(HA) + G(H_3O^+) - G(H_2O) \quad (2)$$

$$HB^+(aq, 1M) + H_2O(1, 1M) \rightarrow H_3O^+(aq, 1M) + B(aq, 1M) \quad (3)$$

$$\Delta G^*_{Diss} = G(B) - G(HB^+) + G(H_3O^+) - G(H_2O) \quad (4)$$

$$pK_a = \Delta G^*_{Diss}/(RT\ \ln(10)) - 1.74 \quad (5)$$

This study is aimed at calculating the pK_a values of three cephalosporin antibiotics (CE), cefapirin (CEFA), cefotaxime (CEFO), and ceftiofur (CEF) by cellmetry method where Eq. 5 including the experimental term was used to calculate the pK values [17–20]. Cellmetry is a newly developed method whereby choosing relevant cell sizes, dissociation, and stability constants can be calculated by plane wave DFT method [21, 22].

✉ Mihály Purgel
purgelmisi@gmail.com

[1] University of Debrecen, Egyetem tér 1, H-4032 Debrecen, Hungary

Published online: 27 March 2024

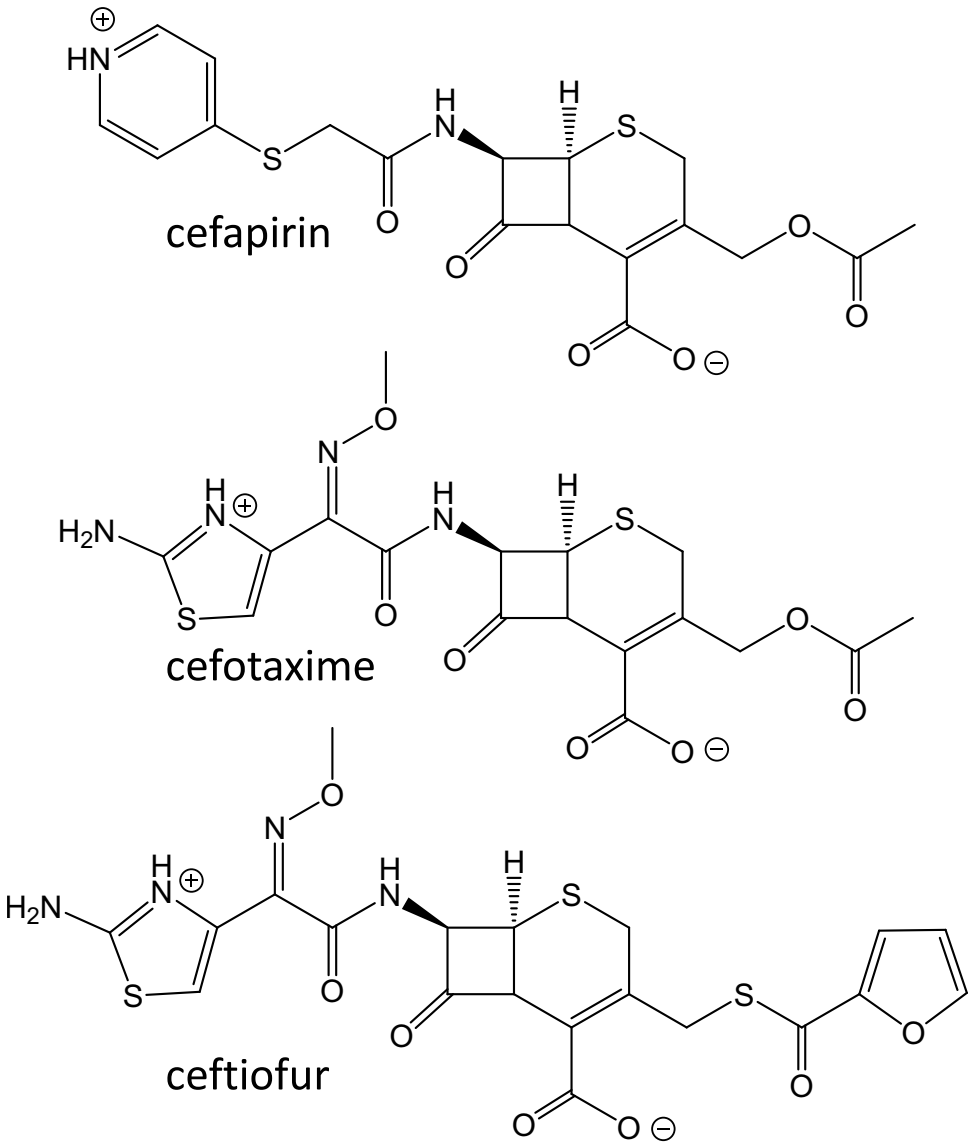

Fig. 1 The zwitter ion form of the cephalosporin antibiotics which were studied

Computational method

Plane-wave density functional theory calculations were carried out using the Quantum Espresso software packages [23–25]. The geometry optimizations were performed with the PBE (Perdew–Burke-Ernzerhof) functional [26, 27], and the Ultrasoft RRKJ (Rabe-Rappe-Kaxiras-Joanoupoulos algorithm) pseudopotential (PP) pseudopotential [https://pseudopotentials.quantum-espresso.org/legacy_tables]. If there was no available _psl.0.1 version of the rrkjus PP, then other _psl.0.2 or _psl.1.0.0 versions were used instead. The Bravais lattice index was 1 (simple or primitive cubic cell), where the k_x, k_y, and k_z points of the Brillouin zone were 1 1 1. The kinetic energy cutoff for wavefunctions (ecutwfc) was 30.0 Rydberg, and the kinetic energy cutoff for charge density and potential for norm-conserving pseudopotential (ecutrho) was 300 Ry. The implicit ENVIRON module described the solvent effect that uses a revised self-consistent continuum solvation model (SCCS) [28–30]. The absolute energies are in Rydberg (1 Rydberg = 0.5; Hartree = 1312.75 kJ mol^{-1}), and the distances are in Bohr (1 Bohr = 0.5292 Ånsgström). Gabedit and Avogadro programs were used to build molecules. The calculated F = E – TS energies are noted in the article as E or energy. The structures of the molecules are represented by the Molekel program.

Results

As a reference, two clusters were defined: the water and hydronium ion together with 3 explicit water molecules optimized at cell size 20 Bohr (Fig. 2). The energies of the acid–base reactions (Eqs. 6 and 7) of the cephalosporin

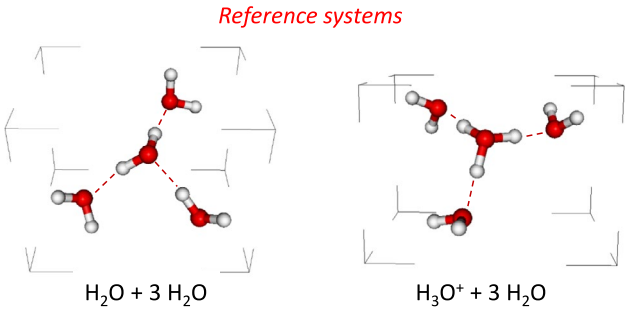

Fig. 2 The structure of the reference clusters optimized at cell size 20 Bohr

antibiotics (CE) were calculated, where HCE^+ is the protonated form of the species, CE^{zw} is the neutral zwitter ion (zw) form, and CE^- is the deprotonated form of the molecules, and the pK values were derived from these energy values according to Eq. 5. For all molecules, the zwitter ion form had significantly lower energy than the non-zw form by ~ 35–45 kJ mol^{-1} in the investigated cell range which would cause ~ 6–8 units pK shift. It also means the minor species had a very small population; therefore, the macroscopic pK only depends on the one derived from zw form.

The size of the three antibiotics is quite different: the distance between the hydrogen atoms which are the furthest from each other is 37.8 Bohr (20 Å) for ceftiofur (CEF), 35 Bohr (18.5 Å) for cefapirin (CEFA), and 33.1 Bohr (17.5 Å) for cefotaxime (CEFO). It was found that the most valuable data were derived in the call range 31–36 Bohr for all species which is in general smaller than the longest distance of the furthest atoms, see above, however, it is worth mentioning that the inside the cell cube the molecule can rotate (turn); therefore, the body (solid) diagonal of the cube is more relevant than its side length. For instance, if cell size was 30 Bohr, then the face diagonal would be 42.4 Bohr as well as the body diagonal would be 52 Bohr. It means that the interstitial region was not too large compared to the atomic core region where the molecule was located.

$$HCE^+ + [4\ H_2O] = CE^{zw} + [H_3O^+ + 3\ H_2O] \quad (6)$$

$$CE^{zw} + [4\ H_2O] = CE^- + [H_3O^+ + 3H_2O] \quad (7)$$

In some cases, the molecules were optimized at certain cell sizes (CS), i.e., in a certain cell range but the cell ranges were also scanned by SCF single-point calculations and the derived pK values were compared to the ones derived from the energies of the optimized geometries. The geometry optimizations were performed using the implicit solvent model.

First, the cefapirin was studied and discussed. Due to the different values obtained by experimental measurements (potentiometry, capillary zone electrophoresis, and UV–Vis spectroscopy), there was a relatively wide range which could be a result of accurate pK value [2, 3, 7, 19–22]. For pK_2 (zwitter ion – deprotonated acid–base pair), there were full geometry optimizations performed at cell size 31, 33–35 Bohr (CS31, CS33–CS35); then, single point calculations were made in a wide cell range using the structures optimized at CS33 and CS34, and the values were compared to each other. We found that at these cell sizes, the values showed accurate values that were smaller than the length of the molecule but significantly shorter than the body diagonal length of the cube. The trendlines derived from single point calculations were almost the same in the cell range 32–42 Bohr, and there was a crossing point of the trendlines around cell size 33 Bohr, but < 32 Bohr, the pK values were different, and this difference was increasing (see Fig. 3). A fine scan was also made where the fractured cell sizes had $\Delta = 0.2$ Bohr, and some characteristic breakpoints were found around 33 and 34 Bohr (see Fig. 3). In the previous study, the calculated pK values of the chosen systems belonged to a breakpoint or a middle point of a characteristic motif of the trendlines. Based on these results, similar calculations were made to determine the pK_1 value, and accurate values were found again at CS33 and CS34; however, the trendlines run together at small cell sizes, and > 33 Bohr, they showed larger differences.

For the larger (longer) ceftiofur (CEF), the trendlines showed some similarities but differences as well (Fig. S1). One would predict that for a larger species, somewhat larger cell size would be reliable according to the differences. If we believe that both pK_1 and pK_2 can be determined at the same call size, then some inconsistencies help us to decide which cell size can be relevant. At CS33 and CS34, the calculated pK values were almost the same, while at CS35, the pK_2 was smaller than pK_1 which could not be correct; however, the calculated pK_1 at CS33 was 1 unit larger than the experimental value. Furthermore, for CEFA, it could be seen that there was a shift, namely, the calc. pK_1 at CS34 was a middle (average) value of the exp. pK_1 range, while the calc. pK_2 was slightly larger than the lowest exp. pK_2 value. According to this phenomenon, the pK_1 can be more accurately estimated at a (slightly) larger cell size.

At this point, the breakpoints could help us to decide, while in the case of CEFA, the characteristic breakpoints appeared for pK_1 at CS34.2 where the lower exp. values were found, while for pK_2, they belonged to the upper exp. values at CS33.2. For pK_1 of CEF, a fine scan was made where the characteristic breakpoint appeared at CS35 (pK = 3.12), the values decreased significantly in the range 35.2–35.6, and the exp. value was in the middle of this section at CS 35.4. Since the breakpoint appeared at CS34 for pK_2 (pK = 3.18), the correct value could be between CS33 and CS34. These values were similar to the ones predicted by Marvin (3.28) and ACD/Percepta (3.60) predictors.

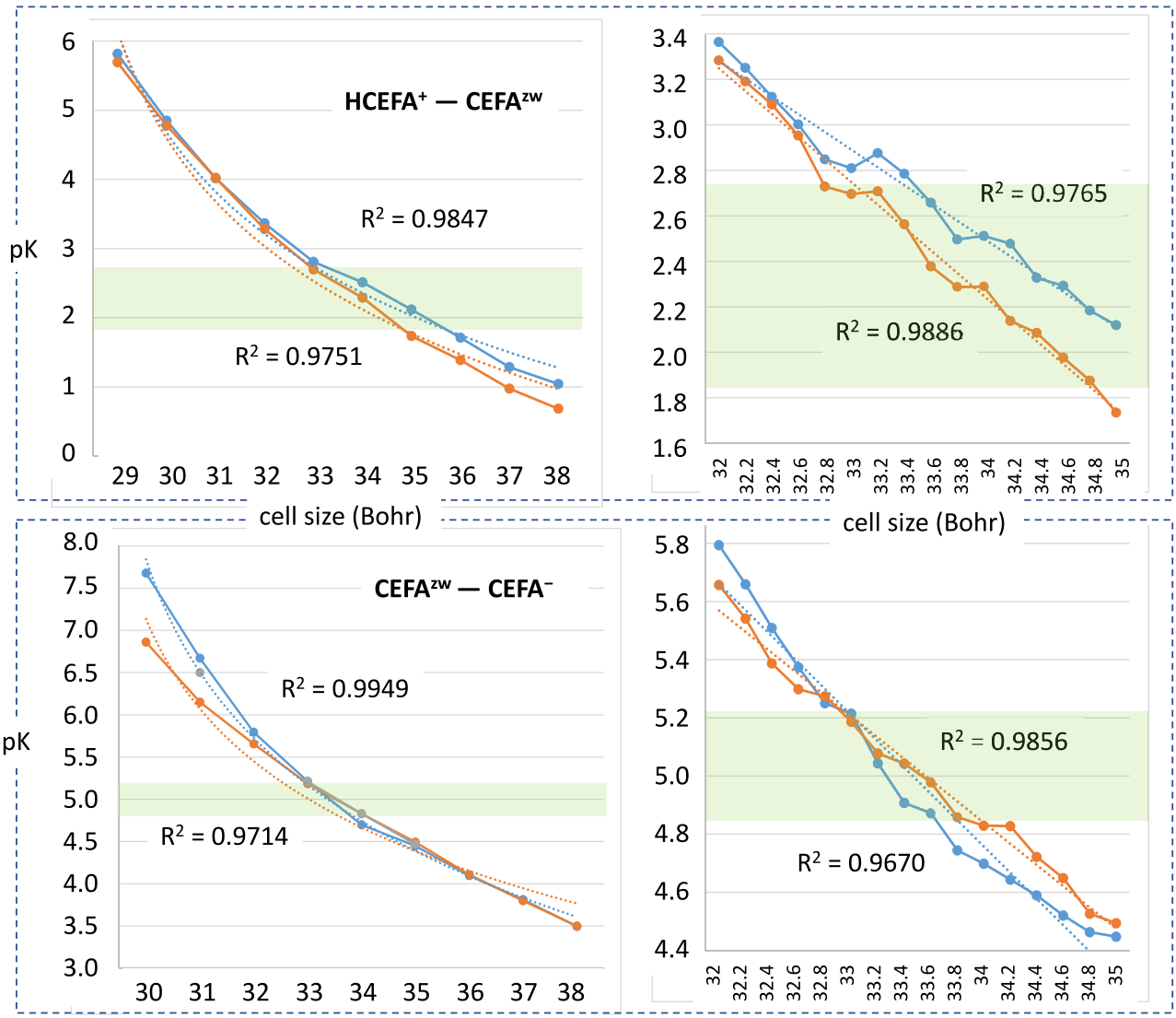

Fig. 3 Trendlines of the equilibria of the CEFA species. The shaded part shows the region of the experimental data. The blue trendlines represent the pK values derived from SCF single point calculations of the optimized geometry at cell size 33 Bohr, while the red points were derived from the optimized structure at 34 Bohr

For the smallest (shortest) cefotaxime, without performing calculations, one could assume that for pK_1 around CS33, while pK_2 around CS32 appears, and these assumptions were confirmed by the calculations. At CS33, 2.24 was calculated for pK_1, and at CS32, 2.97 was calculated for pK_2. A combination of half-unit smaller or larger CS showed also acceptable values: for both pK_1 and pK_2, a slightly underestimated value was calculated at CS 31.5 and a slightly overestimated one at CS 32.5, see Table 1. Interestingly, the curves of the fine scans ($\Delta = 0.2$) made from the optimized structures at 31.5 and 32 Bohr showed a cross point at pK = 3.15 for the equilibrium $CEFO^{zw}$ – $CEFO^-$ which was in the range of the experimental data (see Fig. S2). The $HCEFO^+$ – $CEFO^{zw}$ system showed very different curves derived from the energies of the optimized structures and from the SCF energies of the optimized structures at 32 and 33 Bohr. Obviously, in the pK of the experimental values, breakpoints and a decreasing section of the curves occurred (Fig. S2).

Correction factors were also defined as *the length of the molecule/the cell size resulting in accurate values* where no fractional CS was used except one case. The derived correction values were 0.94 for CEF (pK_1), 0.97 for CEFA (pK_1), 1.0 for CEFO (pK_1), 0.90 for CEF (pK_2), 0.94 for CEFA (pK_2), and 0.97 for CEFO (pK_2), see in Table 1. It can be seen that there was an almost linear trend for the species, and the larger the molecule was, the smaller the correction factor was.

Table 1 The experimental and the calculated acid dissociation constants of the cephalosporins

Antibiotic	Exp. pK_1	Exp. pK_2	Calc. pK_1 (corr. value)	Calc. pK_2
Cefapirin 18.5 Å 35 Bohr	1.85^{P} 2.74^{P}	4.65^{C} 5.13^{UV} 5.44^{UV}	**2.29** CS34 (0.97) **2.81** CS33	**4.83** CS34 **5.21** CS33 (0.94)
Ceftiofur 20 Å 37.8 Bohr	2.68^{P}	No exp (3.28^{Marvin}) ($3.60^{ACD/Percepta}$)	2.32 CS36 **2.69** CS 35.4 (0.94) **3.12** CS35 3.19 CS34 *3.71 CS33*	*2.36* CS35 **3.18** CS34 (0.9) **3.69** CS33
Cefotaxime 17.5 Å 33.1 Bohr	2.09^{C} $2.10–2.90^{P}$	3.20^{C} $3.15–3.40^{P}$	1.69 CS 33.5 **2.24** CS33 (1.0) **3.03** CS 32.5 *3.76* CS32	*2.42* CS 33.5 *2.34 CS33* 2.75 CS 32.5 **2.97** CS32 (0.97) **3.45** CS 31.5

The superscripts assign to the experimental methods where ^{P} is potentiometry, ^{C} is capillary zone electrophoresis, ^{UV} is spectrophotometry. Marvin and ACD/Percepta represent calculated values of ChemAxon's and ACD/Labs' pK_a predictors

Bold numbers represent the best agreement with the experimental values while italic numbers are less relevant ones

Conclusion

The acid dissociation constants of three cephalosporin antibiotics were calculated by the cellmetry methodology. Correlations were found between the size of the molecules and the cell size of the cube which was used for the geometry optimizations, and correction factors were defined which showed a linear trend. It was found that for the major neutral species, the zwitter ion form, and the pK_2, the equilibrium between neutral and deprotonated species needed ~ 1 unit smaller cell sizes than the equilibrium of protonated–neutral species (pK_1). Cellmetry methodology was useful for larger molecules (~ 45–50 atoms) to calculate the acid dissociation constants.

Supplementary Information The online version contains supplementary material available at https://doi.org/10.1007/s11224-024-02312-6.

Acknowledgements The calculations were performed partially on an HP ProLiant DL380 Gen9 server including Intel(R) Xeon(R) CPU E5-2699 v3 @ 2.30GHz processors. Thanks to Dr. Jan H. Schuur for the opportunity to run calculations on his server.

Author contributions CRediT authorship contribution statement Conceptualization: M.S., M.P., Validation: M.S., M.P., Formal analysis: M.S., M.P., Investigation: M.S., M.P., Resources: M.S., M.P., Writing - Original Draft: M.S., M.P., Writing - Review & Editing: M.S., M.P., Visualization: M.S., M.P., Project administration: M.S., M.P., Methodology: M.P. Data Curation: M.P. Supervision: M.P.

Funding Open access funding provided by University of Debrecen.

Data availability Data available on request from the authors.

Declarations

Competing interests The authors declare no competing interests.

References

1. World Health Organization – WHO (2012) Critically important antimicrobials for human medicine - 3rd Rev. Switzerland, Geneva
2. Lin CE, Chen HW, Lin EC, Lin KS, Huang HC (2000) Optimization of separation and migration behavior of cephalosporins in capillary zone electrophoresis. J Chromatogr A 879:197–210
3. Ribeiro AR, Schmidt TC (2017) Determination of acid dissociation constants (pKa) of cephalosporin antibiotics: computational and experimental approaches. Chemosphere 169:524–533
4. Peterson JW, O'Meara TA, Seymour MD, Wang W, Gu B (2009) Sorption mechanisms of cephapirin, a veterinary antibiotic, onto quartz and feldspar minerals as detected by Raman spectroscopy. Environ Pollut 157:1849–1856
5. Sadeghi-Sefidmazgi A, Moradi-Shahrbabak M, Nejati-Javaremi A, Miraei-Ashtiani SR, Amer PR (2011) Estimation of economic

values and financial losses associated with clinical mastitis and somatic cell score in Holstein dairy cattle. Animal 5:33–42
6. Salmon SA, Watts JL, Yancey RJ (1996) In vitro activity of ceftiofur and its primary metabolite, desfuroylceftiofur, against organisms of veterinary importance. J Vet Diagn Invest 8:332–336
7. Streng WH (1977) Microionization constants of commercial cephalosporins. J Pharm Sci 67:666–669
8. Hatanaka T, Morigaki S, Aiba T, Katayama K, Koizumi T (1995) Effect of pH on the skin permeability of a zwitterionic drug, cephalexin. Int J Pharm 125:195–203
9. Lee AC, Crippen GM (2009) Predicting pKa. J Chem Inf Model 49:2013–1033
10. Manchester J, Walkup G, Rivin O, You Z (2010) Evaluation of pKa estimation methods on 211 druglike compounds. J Chem Inf Model 50:565–571
11. Marino EL, Dominguez-Gil A (1981) Determination of the macro-and microionization constants of a dipolar zwitterionic cephalosporin: cefadroxil. Int J Pharm 8:25–33
12. Meloun M, Bordovska S (2007) Benchmarking and validating algorithms that estimate pKa values of drugs based on their molecular structures. Anal Bioanal Chem 389:1267–1281
13. Advanced Chemistry Development Inc., 2016. (ACD/Labs) ACD/PERCEPTA Version 2015. Frankfurt am Main. www.acdlabs.com/pka.
14. ChemAxon, 2016. Marvin, Version 16.2.29. https://chemaxon.com/marvin. Budapest
15. Ho J, Coote ML (2010) A universal approach for continuum solvent pK a calculations: are we there yet? Theor Chem Acc 125:3–21
16. Sckert F, Diedenhofen M, Klamt A (2010) Towards a first principles prediction of pKa: COSMO-RS and the cluster-continuum approach. Mol Phys 108:229–241
17. Purgel M, Schuur JH (2023) Int J Quantum Chem 123:e27042
18. Purgel M, Schuur JH (2023) Int J Quantum Chem 123:e27214
19. Aleksic M, Savic V, Popovic G, Buric N, Kapetanovic V (2005) Acidity constants of cefetamet, cefotaxime and ceftriaxone: the effect of the substituent at C3 position. J Pharm Biomed Anal 39:752–756
20. Andrasi M, Buglyo P, Zekany L, Gaspar A (2007) A comparative study of capillary zone electrophoresis and pH-potentiometry for determination of dissociation constants. J Pharm Biomed Anal 44:1040–1057
21. Fabre H, Eddine NH, Berge G, Blanchin MD (1985) Overlapping ionization constants for cefotaxime. J Pharm Sci 74:84–85
22. Mrestani Y, Neubert R, Munk A, Wiese M (1998) Determination of dissociation constants of cephalosporins by capillary zone electrophoresis. J Chromatogr A 803:273–278
23. Giannozzi P et al (2009) J Phys Condens Matter 21:395502–395520
24. Giannozzi P et al (2017) J Phys Condens Matter 29:465901–465930
25. Giannozzi P et al (2020) J Chem Phys 152:154105–154115
26. Perdew JP, Burke K, Ernzerhof M (1996) Phys Rev Lett 77:3865–3868
27. Perdew JP, Burke K, Ernzerhof M (1997) Phys Rev Lett 78:1396
28. Andreussi O, Dabo I, Marzari N (2012) J Chem Phys 136:064102–064121
29. Dupont C, Andreussi O, Marzari N (2013) J Chem Phys 139:214110–214117
30. Andreussi O, Fisicaro G (2019) Int J Quantum Chem 119:25725–25741